CXCL10 Is Required to Maintain T-Cell Populations and to Control Parasite Replication during Chronic Ocular Toxoplasmosis

Kazumi Norose,[1] *Akitoshi Kikumura,*[1] *Andrew D. Luster,*[2] *Christopher A. Hunter,*[3] *and Tajie H. Harris*[3]

Purpose. *Toxoplasma gondii* is a major cause of ocular disease, which can lead to permanent vision loss in humans. T cells are critically involved in parasite control, but little is known about the molecules that promote T-cell trafficking and migration in the retina. Thus, the aim of this study was to image and dissect the T-cell response during chronic toxoplasmic retinochoroiditis.

Methods. C57BL/6 mice were infected with the Me49 strain of *T. gondii*, and T cells that infiltrated the eye were analyzed by flow cytometry and imaged using multiphoton microscopy. IFN-γ, CXCL9, CXCL10, and CXCR3 mRNA levels were measured by real-time PCR. To investigate the role of CXCL10, mice were treated with anti–CXCL10 antibodies, and histopathology and immunohistochemistry were performed to monitor changes in pathology, cellular infiltration, and parasite burden in the eye.

Results. Infection with *T. gondii* leads to the infiltration of highly activated motile T cells into the eye. These cells express CXCR3 and are capable of producing IFN-γ and TNF-α, and $CD8^+$ T cells express granzyme B. The expression of CXCL9 and CXCL10 in the retina was significantly upregulated during chronic infection. Treatment of chronically infected mice with anti–CXCL10 antibodies led to decreases in the numbers of $CD3^+$, $CD4^+$, and $CD8^+$ T cells and the amount of IFN-γ mRNA expression in the retina and an increase in replicating parasites and ocular pathology.

Conclusions. The maintenance of the T-cell response and the control of *T. gondii* in the eye during chronic infection is dependent on CXCL10. (*Invest Ophthalmol Vis Sci.* 2011;52: 389–398) DOI:10.1167/iovs.10-5819

From the [1]Department of Infection and Host Defense, Graduate School of Medicine, Chiba University, Chiba, Japan; [2]Center for Immunology and Inflammatory Diseases, Division of Rheumatology, Allergy and Immunology, Massachusetts General Hospital, Charlestown, Massachusetts; and [3]Department of Pathobiology, School of Veterinary Medicine, University of Pennsylvania, Philadelphia, Pennsylvania.

Supported by National Institutes of Health Grants AI-41158 (CAH), AI-42334 (CAH), T32-AI-055400 (THH), AI-081478 (THH), R01CA069212 (ADL); the State of Pennsylvania; Japan Society for the Promotion of Science Grant-in-Aid for Scientific Research Grant 20592071 (KN); and the Ministry of Education, Culture, Sports, Science and Technology of Japan (KN).

Submitted for publication May 3, 2010; revised July 20, 2010; accepted August 15, 2010.

Disclosure: **K. Norose**, None; **A. Kikumura**, None; **A.D. Luster**, None; **C.A. Hunter**, None; **T.H. Harris**, None

Corresponding author: Tajie H. Harris, Department of Pathobiology, School of Veterinary Medicine, University of Pennsylvania, 380 S. University Avenue, Philadelphia, PA; tajieh@vet.upenn.edu.

The intracellular, protozoan parasite, *Toxoplasma gondii*, is the most common cause of infectious posterior uveitis worldwide.[1,2] Since approximately one-quarter of the American population and one-third of the world population is chronically infected with *T. gondii*, a significant proportion of the population is at risk for this disease.[3,4] The parasite can be acquired congenitally or, in adults, through the ingestion of food or water contaminated with oocysts or tissue cysts.[4,5] Congenital infections lead to ocular disease in approximately 30% of cases and are associated with active lesions, scarring, and vision loss.[3,6] In adults, the vast majority of acquired infections are asymptomatic, but the suppression of T-cell function associated with long-term corticosteroid treatment, chemotherapy, certain types of cancer, AIDS, and organ transplantation can lead to severe toxoplasmic retinochoroiditis.[2,3,7–10] These patient groups highlight the critical role of T cells in controlling this parasite. However, the development of ocular disease in immunocompetent patients is becoming more prevalent, as illustrated by recent outbreaks in British Columbia and in regions of Brazil.[11,12]

Although treatments are available to limit the replication of *T. gondii* in the eye, parasites are never fully eliminated from this site.[13] As breakdown in the T-cell response can lead to the reemergence of the parasite and the subsequent induction of toxoplasmic retinochoroiditis,[2,3,7–10] it is critical to understand the mechanisms necessary to maintain protective immunity within the eye. Resistance to acute *T. gondii* infection is dependent on the induction of a Th1-polarized immune response that is critically dependent on interferon (IFN)-γ and T cells. Similarly, these factors are necessary for controlling parasite replication in the eye.[14–16] Even though the previous studies highlight the importance of T cells at this local site, the molecules that influence their migration to and within the eye have not been addressed.

One unique facet of T-cell responses in the eye is that immune cell entry is limited under normal conditions because of the blood-retina barrier (BRB). In the presence of local inflammation, lymphocytes cross the BRB in a multistep process that is predicted to be dependent on several molecules, including chemokines.[17,18] Chemokines are a class of molecules that promote the migration of immune cells and, thus, are critically involved in the trafficking of T cells to inflamed tissues. Once T cells enter tissues, it is predicted that chemokines promote T-cell interactions with other immune cells and infected cells.[19] Of particular importance to *T. gondii* infection, CXCL10/IP-10 is an IFN-γ–induced chemokine with potent chemoattractant properties that acts on activated T cells, NK cells, monocytes, and neutrophils.[20] CXCL10 has been reported to play an important role in recruiting activated Th1 cells expressing CXCR3, the receptor for CXCL10, in response to a variety of pathogens.[21–25] Previous work demonstrated that the blockade of

CXCL10 during acute toxoplasmosis prevents T-cell trafficking to liver and spleen, leads to high parasite burdens in the CNS, and causes mice to succumb to infection.[26] Although this work demonstrated the importance of CXCL10 during acute infection, it is unknown whether this chemokine is required to maintain T cell–mediated resistance during chronic ocular toxoplasmosis.

Technical advances in microscopy have allowed for T-cell responses to be visualized in real time in a variety of experimental settings.[19,27] Recently, multiphoton (MP) microscopy studies were performed to characterize T-cell responses during toxoplasmosis, where velocities, trajectories, behavior near parasite-infected cells, and interactions with antigen-presenting cells were observed.[28–31] Intravital microscopy has also been used to identify the molecules necessary for T-cell recruitment to the retina during autoimmune disease,[32–36] but MP microscopy of the T-cell response to *T. gondii* in the eye has not been performed and will allow for further understanding of T-cell responses in this immune-privileged organ.

In this study we investigated the activation status, effector molecule production, and behavior of T cells in the eye during toxoplasmic retinochoroiditis. In addition, a critical role for CXCL10 was identified in the maintenance of T-cell populations and control of *T. gondii* in the eye.

Materials and Methods

Mice, Parasites, and Antibodies

CBA and Swiss Webster mice were obtained from Taconic Farms Inc. (Germantown, NY), and C57BL/6 mice were obtained from Jackson Laboratories (Bar Harbor, ME). DPE^{GFP} transgenic mice that express green fluorescent protein (GFP) in T cells were originally obtained from Ulrich H. von Andrian (CBR, Harvard, Boston MA).[37] GFP expression in DPE^{GFP} mice is driven by the proximal and distal CD4 enhancers and CD4 promoter and lacks the silencer that prevents CD4 expression in mature $CD8^+$ T cells, leading to GFP expression by the majority of T cells. Mice were used between 6 and 8 weeks of age and were housed and bred in specific pathogen-free facilities at the University of Pennsylvania. Mice were handled in accordance with the guidelines of the Institutional Animal Care and Use Committee of the University of Pennsylvania and the ARVO Statement for the Use of Animals in Ophthalmic and Vision Research. The Me49 strain of *T. gondii* was maintained in Swiss Webster mice and passaged into CBA mice to prepare cysts for infection. Age- and sex-matched mice were infected by intraperitoneal injection of 20 cysts in 200 μL PBS. Infection with Me49 strain parasites leads to a disseminated acute infection followed by the establishment of a chronic infection of the eye and brain by days 21 to 28 after inoculation. On days 28, 30, 32, and 34 after infection, 100 μg anti–CXCL10 antibody (1F11)[26] in 300 μL PBS was injected intraperitoneally.

FACS Analysis

Single-cell suspensions were obtained from eyes (six pooled) and spleen by macerating the tissues through 70-μm nylon mesh filters (BD Falcon, Bedford, MA). Spleen samples were subjected to hypotonic red blood cell lysis. The cells were enumerated, and 2×10^6 splenocytes and 2×10^5 cells purified from the eye were resuspended in FACS buffer (1× phosphate-buffered saline, 0.2% bovine serum albumin fraction V, 1 mM EDTA), incubated with F_c block (1 μg/mL 24G2 antibody in FACS buffer), and stained with fixable viability stain (Live/Dead Aqua; Invitrogen, Carlsbad, CA) and conjugated antibodies: CD3-Pacific Blue (BioLegend, San Diego, CA), CD4-eFluor 450, CD8-PerCp Cy5.5, CD45-eFluor 780, CD44-PE-Cy7, CD62L-PE, or CD69-FITC (eBioscience, San Diego, CA) or CXCR3-APC (R&D Systems, Minneapolis, MN). For intracellular cytokine staining, 5×10^5 splenocytes and 2×10^5 cells from the eye were plated in RPMI 1640 (Life Technologies, Gaithersburg, MD) supplemented with 10% fetal calf serum, 1% sodium pyruvate, 1% nonessential amino acids, 0.1% β-mercaptoethanol, 100 U penicillin/mL and 100 μg/mL streptomycin (Gibco, Invitrogen, Grand Island, NY). Cultures were incubated with phorbol myristate acetate (PMA; 100 ng/mL) plus ionomycin (500 ng/mL; Sigma, St. Louis, MO) in the presence of brefeldin A (10 μg/mL; Sigma) for 4 hours at 37°C. After stimulation, cells were surface stained with antibodies specific for CD4 and CD8, fixed with 2% paraformaldehyde (Electron Microscopy Sciences, Hatfield, PA) for 10 minutes, washed, and permeabilized with 0.1% saponin (Sigma) in FACS buffer. Anti–IFN-γ-PerCp Cy5.5, anti–granzyme B-APC, or anti–TNF-α-PE-Cy7 (eBioscience) was added to the cells. Flow cytometry was performed using a flow cytometer (FACSCanto; Becton Dickinson, San Jose, CA), and results were analyzed using FlowJo software (TreeStar Inc., Ashland, OR).

Multiphoton Microscopy

Mice were killed by CO_2 asphyxiation, and the eyes were removed immediately, with minimal mechanical disruption. Whole eye was embedded in 1% agarose (in PBS) in an imaging chamber (Warner Instruments, Hamden, CT). The retina was removed, and retinal whole flat mounts were prepared as described elsewhere.[38] The flat mount retina was placed on a nitrocellulose membrane (Bio-Rad, Hercules, CA) and covered with nylon mesh (Warner Instruments). Specimens were constantly perfused with warm (37°C) oxygenated media (phenol-red free RPMI 1640 supplemented with 10% FBS; Gibco). The temperature in the imaging chamber was maintained at 37°C using heating elements and a temperature control probe. Live ex vivo imaging was performed using a multi-photon microscopy system (SP5; Leica Microsystems, Mannheim, Germany) equipped with a picosecond laser (Coherent Inc., Santa Clara, CA) and external non-descan detectors that allow simultaneous detection of emissions of different wavelengths and second harmonic signals (~460 nm). Enhanced GFP was excited using laser light of 920 nm. Images were obtained using a 20× water-dipping lens. Four-dimensional imaging data were collected by obtaining images from the *x*-, *y*-, and *z*-planes, with a *z*- thickness of approximately 30 μm and a step size of 4 to 5 μm to allow for the capture of a complete *z*-series every 30 seconds for period of 20 minutes. The resultant images were analyzed (Volocity software; PerkinElmer, Waltham, MA). Movies of T-cell migration, mean migratory velocity, and meandering index were calculated using the software.

Real-Time PCR Analysis

Total RNA was extracted from retina using a RNA purification reagent (Trizol; Invitrogen) according to the manufacturer's protocol. Purified RNA was treated with DNase I to eliminate any contamination with genomic DNA (Promega, Madison, WI). cDNA was generated using reverse transcriptase (Superscript II; Invitrogen), and real-time PCR was performed using primers for murine CXCL9/MIG, CXCL10/IP-10, and CXCR3 and normalized to β-actin (QuantiTect; Qiagen, Germantown, MD). IFN-γ expression was measured as previously described.[39] Real-time PCR was performed using a 2× master mix (Power SYBR Green PCR; Applied Biosystems, Warrington, UK) with a PCR system (7500 Fast Real-Time; Applied Bioystems). No template controls were included, and dissociation curve analysis was performed to confirm the specificity of the PCR reactions.

Histopathology and Immunohistochemistry

Sections from formalin-fixed, paraffin-embedded eyes were stained with hematoxylin and eosin and evaluated for inflammatory changes. Each pathologic change was scored on a scale of 0 to 4 as follows: for cellular infiltration in the anterior chamber, vitreous, retina and choroid, scoring system was as follows: 0, no infiltrating cells; 1, <30 inflammatory cells; 2, 30 to 100 inflammatory cells; 3, 100 to 200 inflammatory cells; 4, >200 inflammatory cells. The disorganization of the retinal architecture was scored as follows: 0, normal histology; 1, mild edema; 2, obvious inflammatory reaction and one focal lesion of the retina; 3, few focal lesions with folding of the retinal layers; 4, intensive necrotic retinitis with retinal

destruction or endophthalmitis. Vasculitis was scored as follows: 0, normal histology; 1, vessel dilation; 2, <10 inflammatory cells around the vessels; 3, 10 to 30 inflammatory cells; 4, >30 inflammatory cells. Retinal pigment migration or proliferation was scored as followed: 0, no pigment cells in the retina; 1, <3 pigment cells in the retina; 2, 3 to 10 pigment cells in the retina; 3, 10 to 20 pigment cells in the retina; 4, >20 pigment cells in the retina.

For visualization of GFP^+ cells, eyes were fixed in 10% buffered formalin for 24 hours and then for 24 hours in 30% sucrose, embedded in OCT, and flash frozen. Sections were stained with rabbit anti–GFP (eBiosciences) and rhodamine labeled *Dolichos biflorus* agglutinin (Vector Laboratories, Burlingame, CA) to visualize parasites. For immunohistochemical analysis of infiltrating cells in the retina, eyes were embedded directly in OCT and flash frozen, and 5-μm sagittal sections were cut on a cryostat (CM3050S; Leica). Sections were fixed in 75% acetone and 25% EtOH and were stained using 5 μg/mL rabbit anti–CD3 (Abcam, Cambridge, MA), 5 μg/mL rat anti–mouse CD4, 5 μg/mL rat anti–mouse CD8, 2.5 μg/mL rat anti–mouse CD11b, 12.5 μg/mL hamster anti–mouse CD11c (eBioscience), 2 μg/mL rat-anti–mouse Gr1, 2 μg/mL rat anti–mouse B220, and 2 μg/mL rat anti–mouse I-A/I-E (BD PharMingen). Goat anti–rat Cy3, anti– hamster Cy3 (Jackson ImmunoResearch, West Grove, PA), and anti–rabbit Alexa 488 (Invitrogen) were used as secondary antibodies. Polyclonal rabbit anti–*T. gondii* antibody was generous gift from Fausto G. Araujo (Palo Alto Medical Foundation, Palo Alto, CA). All sections were stained with DAPI (0.5 mg/mL; Invitrogen) to highlight cell nuclei. To control for nonspecific reactions, incubations with an isotype control antibody and reactions without a primary antibody were performed. All images were acquired on a microscope (E600; Nikon, Melville, NY) equipped with a charge-coupled device camera (CoolSNAP; Photometrics, Tucson, AZ) for fluorescence microscopy and a digital camera (DS-Fi1Nikon) for light microscopy. Images were processed with imaging software (NIS Elements; Nikon). For parasite enumeration by immunohistochemistry, sections of retina with a total depth of 180 to 200 μm were examined from each mouse.

Statistical Analysis

Results of experimental studies are reported as mean ± SE. Differences were analyzed using the Student's *t*-test or Mann-Whitney *U* test. $P < 0.05$ was regarded as significant.

Results

T-Cell Responses in the Eye during Chronic Ocular Toxoplasmosis

Although it has been demonstrated that T cells are required for optimal control of ocular toxoplasmosis,[14–16] relatively little is known about the characteristics of the T cells at this site. Therefore, C57BL/6 mice were infected for 35 days with the Me49 strain *T. gondii*, and flow cytometry was performed on cells isolated from the eye and compared to cells from the spleen. T cells were identified from live cells isolated from the eye by CD45 (Fig. 1A) and CD3 expression (Fig. 1B). Of the $CD3^+$ cells in the eye, most were $CD4^+$ (Fig. 1C). Fewer than 10 T cells were isolated from an uninfected eye (data not shown), whereas $CD4^+$ and $CD8^+$ T cells were approximately 33% of the live cells isolated from infected eyes (Fig. 1D). The T cells in the eye were highly activated, as assessed by high expression of CD44 and low levels of CD62L (Fig. 1E). $CD4^+$ T cells were uniformly $CD62L^{lo}$, and only 2% of the $CD8^+$ T cells expressed CD62L. In addition, approximately 80% of the cells expressed CD69, a marker of recent activation (Fig. 1F). In comparison, 50% of the $CD4^+$ and $CD8^+$ T cells in the spleen were $CD44^{hi}$ $CD62^{lo}$ and <20% were $CD69^+$ during chronic infection (data not shown). These results are consistent with previous observations that

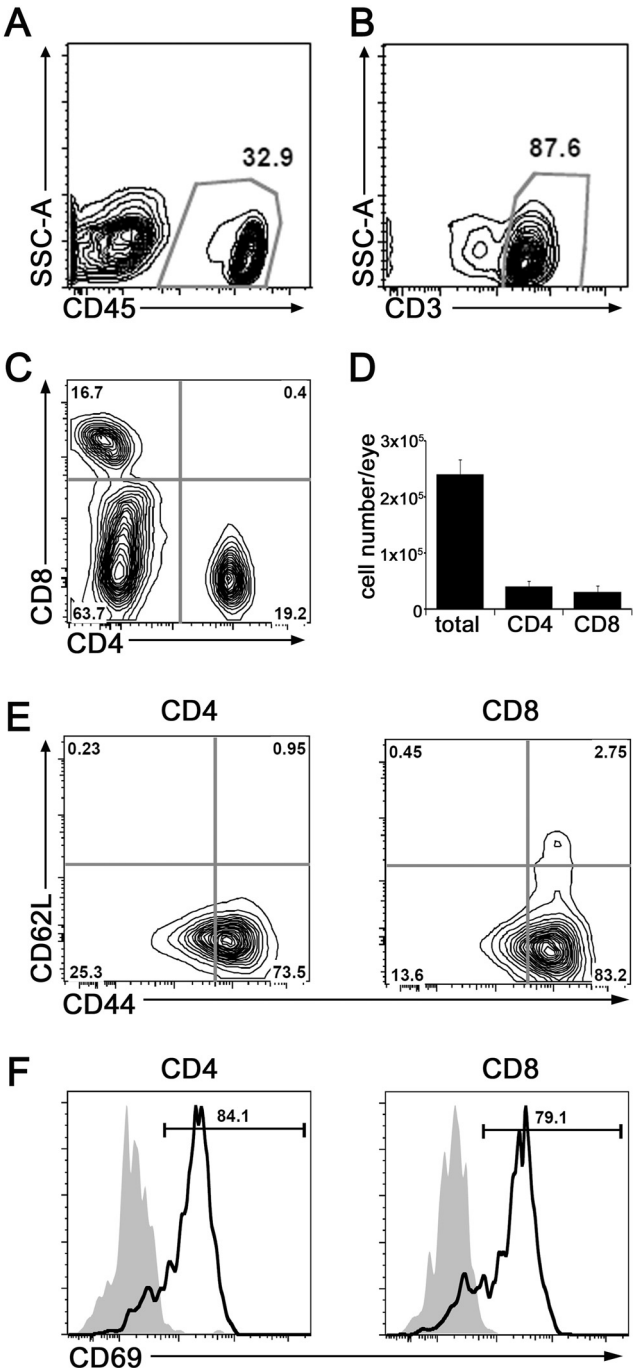

Figure 1. T cells isolated from the eye during ocular toxoplasmosis are highly activated. Cells were isolated from infected eyes and analyzed by flow cytometry. CD45 expression was analyzed on live cells isolated from the eye (**A**). $CD45^+$ cells were analyzed for CD3 expression (**B**) and subsequently gated on CD4 and CD8 expression (**C**). The total number of live cells (total) and $CD4^+$ and $CD8^+$ T cells are presented as mean ± SE from four independent experiments (**D**). CD44 and CD62L (**E**) and CD69 expression (**F**) on T cells isolated from infected eyes are shown. *Shaded* histogram represents fluorescence minus one control. All plots are representative of three independent experiments with a minimum of three mice per group.

cells that infiltrate the eye during autoimmune uveoretinitis display a highly activated phenotype.[35,40]

To determine whether these T cells acquire effector functions in response to *T. gondii*, intracellular cytokine staining was performed to assess levels of TNF-α, IFN-γ, and granzyme

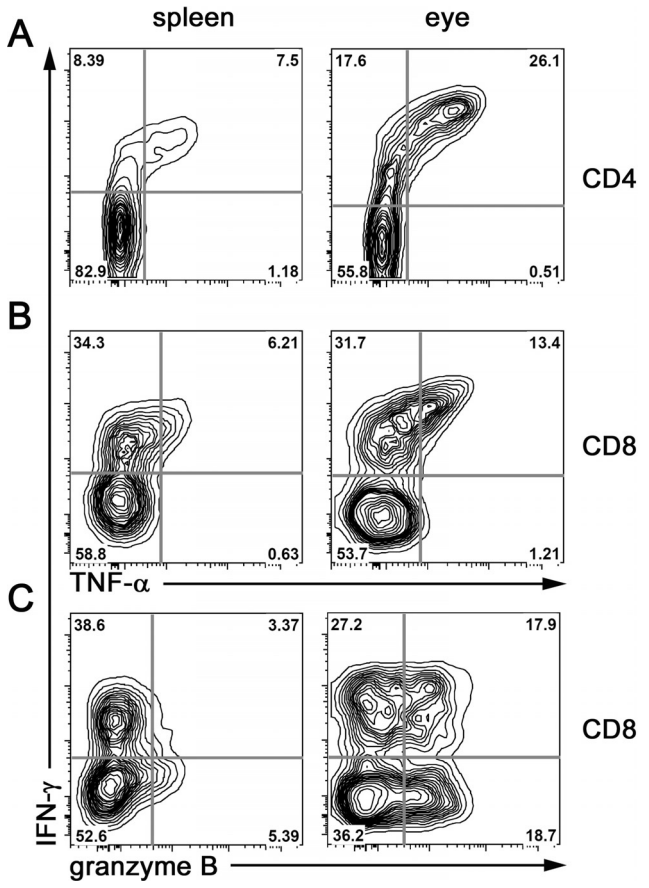

FIGURE 2. T cells isolated from the eye during ocular toxoplasmosis produce effector cytokines and lytic granules. Ex vivo cytokine production by T cells from the spleen and eye was assessed by flow cytometry. TNF-α and IFN-γ production was assessed in $CD4^+$ cells (**A**) and $CD8^+$ cells (**B**). Granzyme and IFN-γ production was measured in $CD8^+$ T cells (**C**). Graphs are representative of three independent experiments with a minimum of three mice per group.

production. In the eyes of infected mice, a higher percentage of $CD4^+$ T and $CD8^+$ T cells were making effector cytokines in comparison to the spleen (Figs. 2A, 2B). Although a higher percentage of $CD8^+$ T cells were making IFN-γ at this time point, $CD4^+$ T cells tended to be double producers of TNF-α and IFN-γ more often than $CD8^+$ T cells (Figs. 2A, 2B). Interestingly, every TNF-α–producing cell was also making IFN-γ. $CD8^+$ T cells in the eye were making far more granzyme B than cells in the spleen and cells were making granzyme B alone, IFN-γ alone, or both molecules, suggesting that not all cytokine-producing cells are also cytolytic (Fig. 2C). Together, these data reveal that chronic infection of the eye with *T. gondii* is characterized by the presence of highly activated $CD4^+$ and $CD8^+$ T cells that express cytokines and effector molecules, consistent with the presence of an ongoing local T-cell response.

Visualizing T-Cell Behavior during Ocular Toxoplasmosis

The behavior of $CD8^+$ T cells in the lymph node and brain during *T. gondii* infection has been visualized by MP microscopy. To assess whether T-cell behavior during toxoplasmic retinochoroiditis could be visualized by MP microscopy, transgenic mice expressing GFP in all T cells (DPE^{GFP}) were infected with *T. gondii*. In uninfected mice, no GFP^+ T cells were observed in the eyes. On day 32 after infection, flow cytometric analysis showed that GFP^+ T cells were present in the eyes of infected mice (Fig. 3A) and the percentage of GFP^+ $CD4^+$ T cells was much higher than that of GFP^+ $CD8^+$ T cells (Fig. 3B), though the percentage of GFP^+ $CD4^+$ and $CD8^+$ T cells in the spleen was equal (data not shown). Histologic analysis revealed that the GFP^+ T cells were found near *T. gondii* cysts in the retina (Fig. 3C).

Next, MP microscopy was used to visualize the behavior of endogenous GFP^+ T lymphocyte populations in the retina and iris of DPE^{GFP} mice chronically infected with *T. gondii*. This approach revealed a large GFP^+ population in both of these sites (Fig. 3D and Supplementary Movies S1 and S2, http://www.iovs.org/lookup/suppl/doi:10.1167/iovs.10-5819/-/DCSupplemental). Tracking of individual T cells was performed to determine the cell velocity (distance/time) and meandering index (displacement from origin [μm]/track length [μm]). Sample cell tracks of GFP^+ T cells during an imaging session are shown in Figure 3D. Individual cell analysis revealed an average velocity of 4.08 μm/min in the retina and iris, but these cells moved at a wide range of speeds, and cells in the iris moved with the highest velocity (>20 μm/min; Fig. 3E). Immobile T cells that were round—a morphology consistent with T-cell engagement with cells presenting cognate antigen—were also observed. This observation suggests that T cells within the eye interacted with other immune cells, such as antigen-presenting cells, or infected cells presenting *T. gondii* antigen. The average meandering index, a ratio of the distance traveled to the overall displacement of the cell, showed that GFP^+ T cells in the iris migrated in straighter paths than those in the retina (0.368 ± 0.28 vs. 0.28 ± 0.21; $P = 0.02$; Fig. 3F). Together, these analyses demonstrate that T cells display a variety of migratory behaviors in the infected retina and that MP microscopy is a tool that can be used to dissect the biology of the T-cell response to parasite infection of the retina.

Chemokine and Chemokine Receptor Expression during Ocular Toxoplasmosis

To identify factors that may influence T-cell recruitment and migration in the eye during chronic *T. gondii* infection, chemokine expression in the infected retina was assessed by real-time PCR. CXCL9 and CXCL10 are IFN-γ–induced chemokines that are the ligands for CXCR3, a receptor associated with the trafficking of Th1 cells in response to infection. The levels of IFN-γ, CXCL9, CXCL10, and CXCR3 mRNA in the retina was measured by real-time PCR and compared with uninfected controls. These genes were highly expressed after infection, with approximately 500-fold induction of IFN-γ mRNA, 8000-fold increase in CXCL9 mRNA, 800-fold increase in CXCL10 mRNA, and 800-fold increase in CXCR3 mRNA (Fig. 4A). Flow cytometric analysis also revealed that greater than 50% of the $CD4^+$ and $CD8^+$ T cells in the spleen and eye express CXCR3, with more $CD4^+$ cells expressing CXCR3 than $CD8^+$ cells (Fig. 4B). Thus, these data suggest that these chemokines and chemokine receptor likely influence the T cell response to *T. gondii* in the retina.

CXCL10 Neutralization Leads to Increased Ocular Pathology and Decreased T-Cell Numbers in the Retina

To determine the role of CXCL10 during chronic ocular toxoplasmosis, mice were infected for 28 days to allow for the development of ocular infection and were subsequently treated with anti–CXCL10 antibodies for 7 days. After anti–CXCL10 treatment, a histologic assessment (as described in Materials and Methods) of the eye was performed. Thirteen eyes from the control groups and 11 eyes from the antibody-treated groups

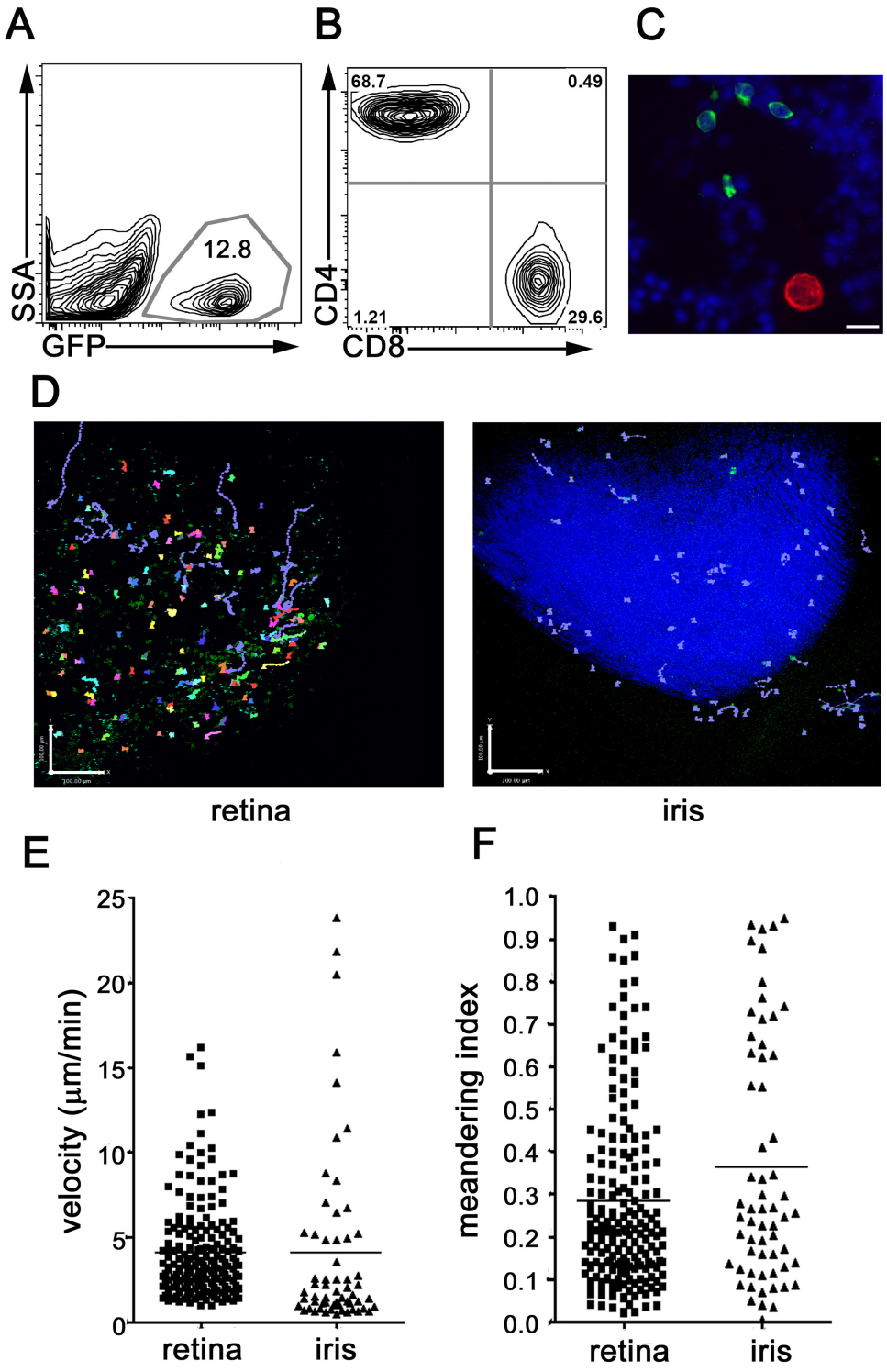

FIGURE 3. MP imaging of T cells in the eye reveals heterogeneity in behavior. (**A**) GFP expression in the eye was evaluated by flow cytometry. (**B**) GFP-expressing cells were analyzed for CD4 and CD8 expression. (**C**) Immunohistochemistry revealed that GFP^+ T cells (*green*) were found in proximity to a *T. gondii* cyst (*red*). Scale bar, 10 μm. GFP^+ T-cell behavior in the eye was imaged using MP microscopy. (**D**) GFP^+ cells (*green*), secondary harmonic emitting structures (*blue*), and example cells tracks (*multicolored lines*) are shown from the retina (*left*) and iris (*right*). Images were collected to generate four-dimensional (*x-*, *y-*, and *z-* planes over time) analysis of T-cell migration. Scale bars, 100 μm. Individual cells were analyzed for (**E**) mean velocity and (**F**) meandering index. Retina, $n = 192$ cells; iris, $n = 60$ cells. Graphs are representative of three independent experiments.

from three independent experiments were examined. In mice treated with control antibodies, cellular infiltration into the anterior chamber, vitreous, retina, and the synechiae of the iris and lens was observed (Fig. 5A2–4). After anti–CXCL10 treatment, there were increases in inflammatory cell infiltration in the retinal perivascular region, neuroretina, and choroid and significantly more disorganization of the normal architecture in the comparison to the control (Fig. 5A5–7, 5B). The disorganization of the retinal structure in the treated mice was more severe than that in the control mice.

To determine whether CXCL10 neutralization affected immune cell populations in the retina, we analyzed the retina by immunohistochemistry on day 35 after infection. Immune cells were not detected in the retina of naive mice (data not shown). After infection, $CD3^+$, $CD4^+$, and $CD8^+$ lymphocyte populations were observed in the retina (Fig. 6A). In addition to T cells, $CD11b^+$, $CD11c^+$, major histocompatibility complex class II^+, and $Gr1^+$ cells were detected, highlighting the marked changes in the retina induced by *T. gondii* infection. Anti–CXCL10 treatment led to significant decreases in $CD4^+$ T cells (Fig. 6B; $P = 0.041$), but no

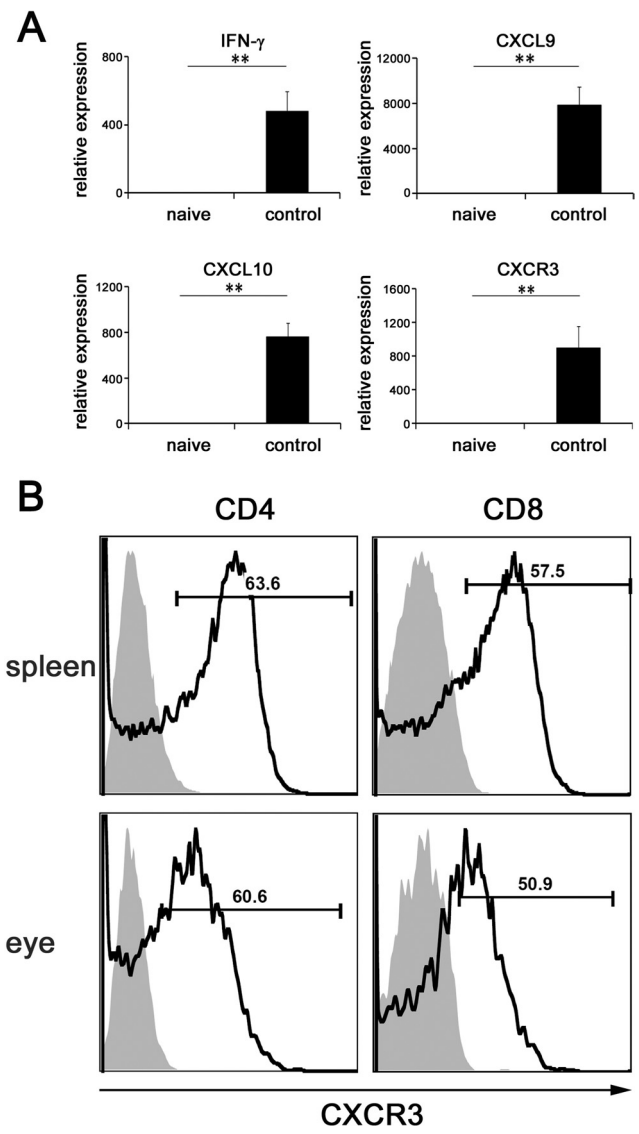

FIGURE 4. IFN-γ–dependent, T cell-associated chemokines and chemokine receptors are expressed in the retina during chronic *T. gondii* infection. Retinas were isolated from chronically infected mice, and gene expression was analyzed by real-time PCR. (**A**) IFN-γ, CXCL9, CXCL10, and CXCR3 expression was measured by real-time PCR. Levels were normalized to β-actin, and the results are depicted as fold increase over retinas from uninfected mice. $^{**}P < 0.01$. (**B**) CXCR3 expression on T cells isolated from the spleen and eye was determined by flow cytometry. *Shaded* histograms represent fluorescence minus one control. Plots are representative of three independent experiments.

changes were detected in other infiltrating cell populations. Together these results suggest that the maintenance of $CD4^+$ T cell populations in the eye requires CXCL10.

Anti–CXCL10 Treatment Causes Decreases in IFN-γ mRNA Expression and Increases in Parasite Replication

Because T cells are a source of IFN-γ in the eye, the effect of anti–CXCL10 treatment on IFN-γ mRNA expression in the retina was measured by real-time PCR. Levels of IFN-γ message were reduced after chemokine blockade (Fig. 6C; $P = 0.063$), suggesting that CXCL10 is necessary to maintain local IFN-γ production in the eye. Given the critical role of IFN-γ in the control of *T. gondii* replication, the effect of anti–CXCL10 treatment on parasite burden was assessed using immunohistochemistry. Analysis revealed that parasites in the eyes of control mice were entirely in cyst form (Fig. 6D1). Parasites in the retinas of anti–CXCL10-treated mice were found in cyst form (Fig. 6D2), and the replicative tachyzoite form parasites (negative for *Dolichos*-binding lectin) were observed, consistent with reactivation (Fig. 6D3). To enumerate changes in parasite burden within the retina, sections were scored for the presence of parasites. A focal region of parasite infection, such as an intact cyst or a group of tachyzoites, was considered a region of *T. gondii*. Significantly more regions of parasites were present in anti–CXCL10-treated mice than in control mice (Fig. 6E), suggesting that decreases in T cell–derived IFN-γ after anti–CXCL10 treatment leads to the reactivation of latent parasite cysts. Moreover, it is likely that the observed parasite reactivation may underlie the increase in ocular pathology observed in anti–CXCL10 treated mice.

DISCUSSION

The importance of T cells in maintaining resistance to chronic *T. gondii* infection, including ocular infection, has been highlighted in several studies.[14–16,41] Despite their importance as a critical component of resistance to ocular disease, current understanding of the effector functions of T cells in the eye and the molecules required to support this response remain limited.[6,42] In the present study, the phenotypic analysis of infiltrating T cells indicated that these cells were highly activated effector cells, consistent with the idea that a local T-cell response is required to control *T. gondii* in the eye. Previous studies have also demonstrated the importance of TNF-α and IFN-γ during chronic ocular toxoplasmosis.[14] This study confirms that T cells are producers of these key cytokines. In addition, approximately 50% of $CD8^+$ T cells in the eye produced high levels of granzyme B, indicating that they are likely cytolytic effector cells. Given that many studies on chronic *T. gondii* infection have focused on the brain, it would be of interest to revisit studies using perforin- or granzyme-deficient mice to explore the role of $CD8^+$ T cell–mediated cytolysis during chronic ocular toxoplasmosis.

MP microscopy has been used to image the behavior of $CD8^+$ T cells in the brain and lymph nodes during *T. gondii* infection.[28,30,31] In the present study, polyclonal $CD4^+$ and $CD8^+$ T cells were imaged in the retina and iris of chronically infected mice. The GFP-expressing T cells had equivalent mean velocities in the retina and the iris, although the fastest migrating cells were observed in the iris. Additionally, T cells in the iris migrated along straighter paths than did cells in the retina. Several factors likely influence T-cell migration in the eye during chronic *T. gondii* infection and may explain any differences in behavior observed between the iris and the retina. For example *T. gondii* parasites have not been detected in the iris in this study or others.[43] Given that cognate antigen presentation to T cells provides a "stop signal,"[44,45] a low level or an absence of antigen may lead to enhanced T-cell speeds. Although the current analysis of T-cell behavior did not distinguish between $CD4^+$ and $CD8^+$ T cells, these studies demonstrated the feasibility of imaging the T-cell response to *T. gondii* in the eye. The application and refinement of this approach will help address the fundamental questions of how T cells are recruited and retained within the tissues, how T cells interact with antigen-presenting cells, and whether $CD8^+$ T cells directly limit parasite replication by the lysis of infected cells.[18,27]

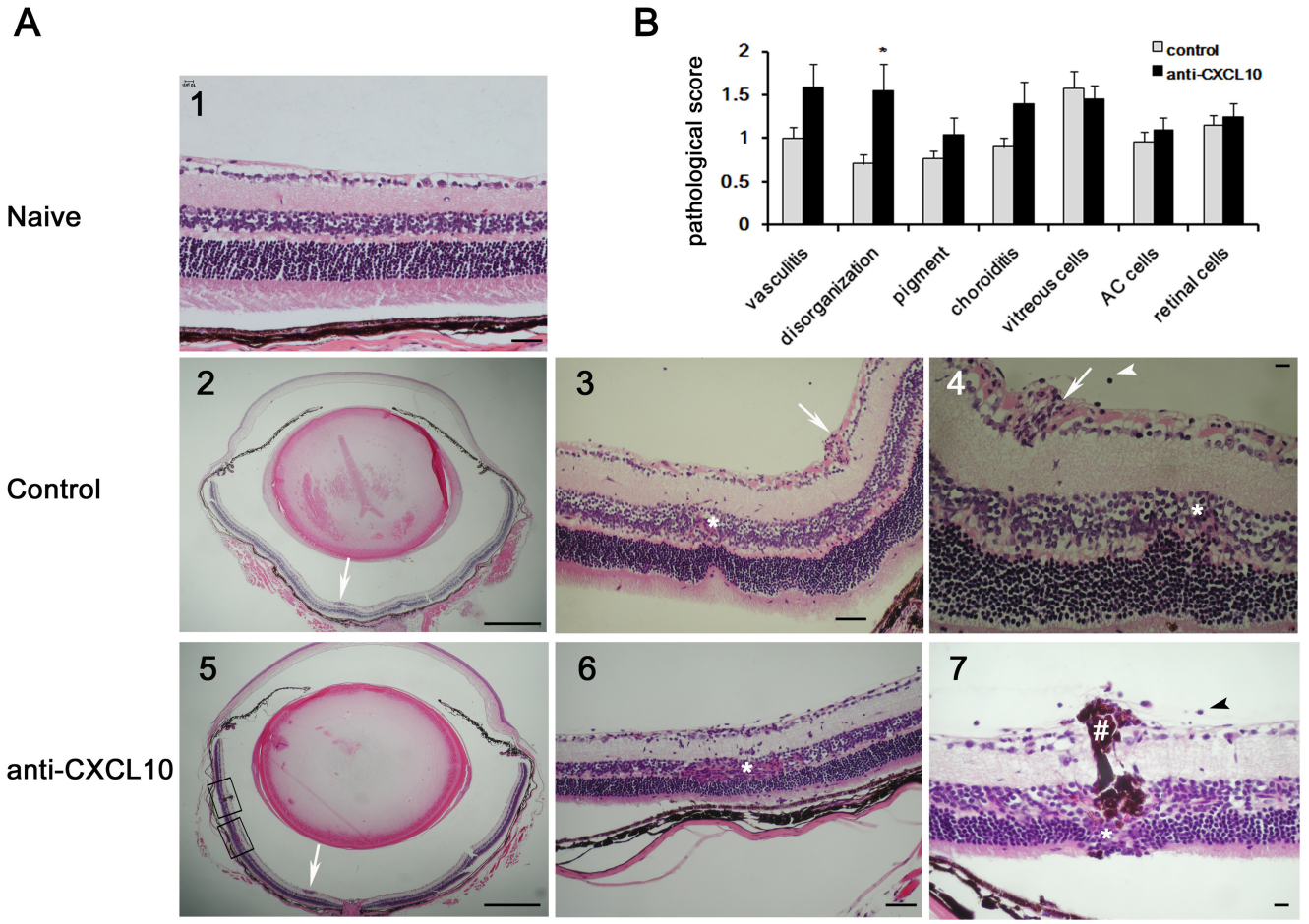

FIGURE 5. CXCL10 neutralization during chronic ocular toxoplasmosis causes increased pathology in the eye. (**A**) Representative images from hematoxylin and eosin–stained retinas from naive, (**1**) infected control mice, (**2**–**4**) and infected mice treated with anti–CXCL10 antibodies. (**5**–**7**) Magnified regions from image (**5**) are indicated by *black boxes* and are shown in images (**6**) and (**7**). Examples of vasculitis (*arrows*), disorganization of the normal retinal structure (*asterisks*), inflammatory cell infiltration in the vitreous (*arrowhead*), and retinal pigment epithelium (#) were noted. Scale bars: 50 μm (**1**, **3**, **6**); 500 μm (**2**, **5**); 10 μm (**4**, **7**). (**B**) A pathology score was determined for control and anti–CXCL10-treated mice with the following parameters: cell infiltration in retinal perivascular region (vasculitis), disorganization of the retinal architecture (disorganization), retinal pigment epithelium migration or proliferation (pigment), and cell infiltration in the choroid (choroiditis), vitreous (vitreous cells), anterior chamber (AC cells), and retina (retinal cells). $^{*}P < 0.05$. Mean pathology score ± SE from three independent experiments is shown ($n = 13$ for control and $n = 11$ for anti–CXCL10 treated mice).

In this study, neutralization of CXCL10 during the chronic stage resulted in the disorganization of the retinal architecture and a significant decrease in $CD4^+$ T cells. Because a higher percentage of $CD4^+$ T cells than $CD8^+$ T cells isolated from the eye express CXCR3, they may be more sensitive to CXCL10 blockade than $CD8^+$ T cells. As $CD4^+$ T cells produce TNF-α and IFN-γ, the effects of neutralizing CXCL10 might lead to the reactivation of parasite cysts, leading to increased pathology. In addition to CXCR3 expression on cytokine-producing effector cells, it has been demonstrated that CXCR3 is required for $CD4^+$ regulatory T cells (Tregs) to traffic to specific regions of the brain and to limit pathology during experimental autoimmune encephalomyelitis.[46] Thus, a decrease in $CD4^+$ Tregs may be caused by CXCL10 blockade, leading to increased immune pathology. Although it is tempting to conclude that anti–CXCL10 treatment prevents the recruitment of $CD4^+$ T cells into the retina, these studies do not distinguish between CXCL10-dependent recruitment and retention in the retina. Nevertheless, the maintenance of the $CD4^+$ T-cell population in the retina during chronic infection is CXCL10 dependent. Future MP imaging experiments will be required to distinguish between these possibilities.

Although this study focused on the role of CXCL10, it is of interest whether CXCL9, a CXCR3 ligand, also affects the T-cell response in the eye. In a study focused on chemokine expression in the brain during chronic toxoplasmosis, CXCL9 and CXCL10, respectively, were produced by infiltrating macrophages and astrocytes, supporting the hypothesis that the differential expression of CXCR3 ligands may lead to a unique function of each chemokine.[47,48] Future studies will be carried out to address the cellular source of these chemokines in the retina. In addition, specific blocking reagents for CXCL9 and CXCR3 could be used to differentiate the role of individual and additive roles of these chemokines. It is likely that chemokines other than CXCR3 ligands—such as CCR5, which has also been reported to be required for optimal control of *T. gondii*—are necessary to support the T-cell response to ocular toxoplasmosis.[49]

Recruitment of T lymphocytes into the eye during autoimmune reactions can lead to severe pathology.[18,50] Thus, it has been proposed that targeting the molecules that promote T-cell responses in the eye, including chemokines, may provide therapeutic approaches to manage T cell–mediated inflammatory conditions such as multiple sclerosis.[51–53] One possible adverse affect is that inhibition of chemokines would likely antagonize T-cell responses during chronic toxoplasmosis. Recently, a patient with

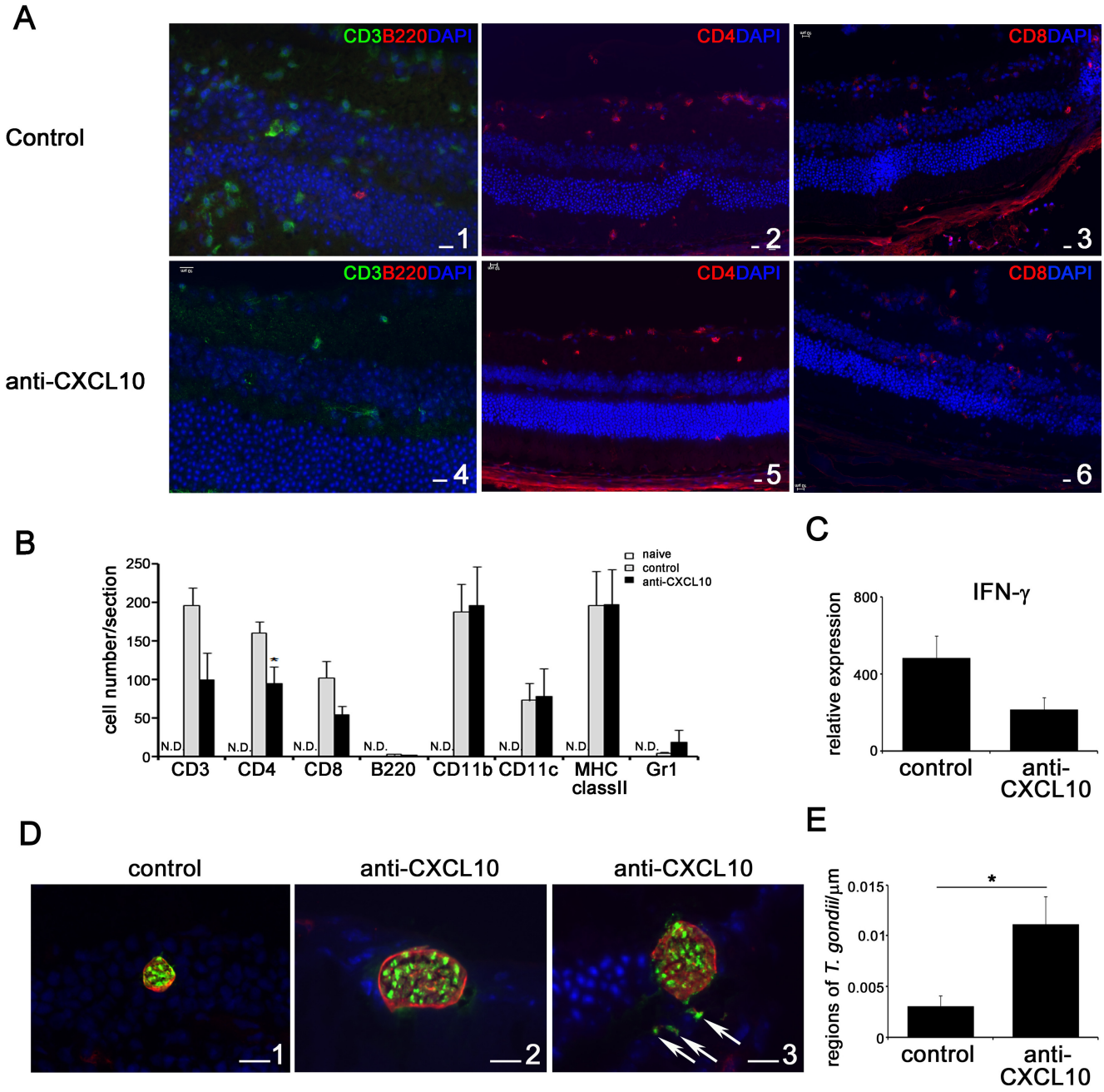

Figure 6. CXCL10 is required to maintain T-cell populations, IFN-γ mRNA expression, and parasite control in the retina during chronic *T. gondii* infection. (**A**) Images from immunohistochemical analysis of retinas from control treated *T. gondii*–infected mice (**A1–3**) and anti–CXCL10 treatment (**A4–6**) are shown. Sections were stained for $CD3^+$ (*green*) and $B220^+$ (*red*; **A1**, **A4**) cells, $CD4^+$ cells (*red*; **A2**, **A5**), and $CD8^+$ cells (*red*; **A3**, **A6**), and nuclei were stained with DAPI (*blue*). Scale bars, 10 μm. Numbers of various cell types in the retina in control and anti–CXCL10 treated mice were compiled from the immunohistochemical analysis, and the data are presented as the mean ± SE ($n = 5$) from three independent experiments. N.D., not detected (**B**). IFN-γ expression was measured by real-time PCR from the retinas of control and anti–CXCL10-treated mice (**C**). *T. gondii* parasites in the retina were examined by immunohistochemistry using anti–*T. gondii* antibodies (*green*) and *Dolichos*-binding lectin (*red*; **D**). All parasites in control mice were found in intact cysts (**D1**). Parasites in anti–CXCL10-treated mice were found in cyst form (**D2**) and tachyzoite form (*arrows*; **D3**). Scale bars, 10 μm. (**E**) Regions of *T. gondii* parasites (cysts or free parasites) in the retinas of control and anti–CXCL10-treated mice were enumerated from sections totaling 180 to 200 μm in depth. Data are expressed as the average number of parasite regions per tissue depth (μm) from eight control and six anti–CXCL10-treated mice. Data are presented as mean ± SE. $^*P < 0.05$.

multiple sclerosis undergoing natalizumab treatment to block α_4-integrin–mediated T-cell recruitment developed severe ocular toxoplasmosis.[7] Taken together, further understanding of the molecules that support T cell–mediated resistance to chronic *T. gondii* infection may inform drug choice and development to avoid the unwanted reactivation of latent *T. gondii*.

Acknowledgments

The authors thank Lingli Zhang of the University of Pennsylvania Veterinary Imaging Facility for her assistance with multiphoton microscopy studies and Elia Tait for her help with flow cytometric analyses.

References

1. McCannel CA, Holland GN, Helm CJ, Cornell PJ, Winston JV, Rimmer TG. Causes of uveitis in the general practice of ophthalmology: UCLA Community-Based Uveitis Study Group. *Am J Ophthalmol.* 1996;121:35–46.
2. Hooper C, McCluskey P. Intraocular inflammation: its causes and investigations. *Curr Allergy Asthma Rep.* 2008;8:331–338.
3. Holland GN. Reconsidering the pathogenesis of ocular toxoplasmosis. *Am J Ophthalmol.* 1999;128:502–505.
4. Jones JL, Dargelas V, Roberts J, Press C, Remington JS, Montoya JG. Risk factors for *Toxoplasma gondii* infection in the United States. *Clin Infect Dis.* 2009;49:878–884.
5. Dubey JP, Jones JL. *Toxoplasma gondii* infection in humans and animals in the United States. *Int J Parasitol.* 2008;38:1257–1278.
6. Jones LA, Alexander J, Roberts CW. Ocular toxoplasmosis: in the storm of the eye. *Parasite Immunol.* 2006;28:635–642.
7. Zecca C, Nessi F, Bernasconi E, Gobbi C. Ocular toxoplasmosis during natalizumab treatment. *Neurology.* 2009;73:1418–1419.
8. Holland GN. Ocular toxoplasmosis: the influence of patient age. *Mem Inst Oswaldo Cruz.* 2009;104:351–357.
9. Holland GN, Crespi CM, ten Dam-van Loon N, et al. Analysis of recurrence patterns associated with toxoplasmic retinochoroiditis. *Am J Ophthalmol.* 2008;145:1007–1013.
10. Holland GN, Engstrom RE Jr, Glasgow BJ, et al. Ocular toxoplasmosis in patients with the acquired immunodeficiency syndrome. *Am J Ophthalmol.* 1988;106:653–667.
11. Glasner PD, Silveira C, Kruszon-Moran D, et al. An unusually high prevalence of ocular toxoplasmosis in southern Brazil. *Am J Ophthalmol.* 1992;114:136–144.
12. Burnett AJ, Shortt SG, Isaac-Renton J, King A, Werker D, Bowie WR. Multiple cases of acquired toxoplasmosis retinitis presenting in an outbreak. *Ophthalmology.* 1998;105:1032–1037.
13. Bonfioli AA, Orefice F. Toxoplasmosis. *Semin Ophthalmol.* 2005; 20:129–141.
14. Gazzinelli RT, Brezin A, Li Q, Nussenblatt RB, Chan CC. *Toxoplasma gondii*: acquired ocular toxoplasmosis in the murine model, protective role of TNF-alpha and IFN-gamma. *Exp Parasitol.* 1994;78:217–229.
15. Lu F, Huang S, Kasper LH. The temperature-sensitive mutants of *Toxoplasma gondii* and ocular toxoplasmosis. *Vaccine.* 2009;27: 573–580.
16. Lu F, Huang S, Kasper LH. CD4+ T cells in the pathogenesis of murine ocular toxoplasmosis. *Infect Immun.* 2004;72:4966–4972.
17. Crane IJ, Liversidge J. Mechanisms of leukocyte migration across the blood-retina barrier. *Semin Immunopathol.* 2008;30:165–177.
18. Caspi RR. Ocular autoimmunity: the price of privilege? *Immunol Rev.* 2006;213:23–35.
19. Bromley SK, Mempel TR, Luster AD. Orchestrating the orchestrators: chemokines in control of T cell traffic. *Nat Immunol.* 2008;9:970–980.
20. Cyster JG. Chemokines, sphingosine-1-phosphate, and cell migration in secondary lymphoid organs. *Annu Rev Immunol.* 2005;23: 127–159.
21. Liu L, Callahan MK, Huang D, Ransohoff RM. Chemokine receptor CXCR3: an unexpected enigma. *Curr Top Dev Biol.* 2005;68:149–181.
22. Stiles LN, Hosking MP, Edwards RA, Strieter RM, Lane TE. Differential roles for CXCR3 in CD4+ and CD8+ T cell trafficking following viral infection of the CNS. *Eur J Immunol.* 2006;36:613–622.
23. Zhang B, Chan YK, Lu B, Diamond MS, Klein RS. CXCR3 mediates region-specific antiviral t cell trafficking within the central nervous system during West Nile virus encephalitis. *J Immunol.* 2008;180: 2641–2649.
24. de Lemos C, Christensen JE, Nansen A, et al. Opposing effects of CXCR3 and CCR5 deficiency on CD8+ T cell-mediated inflammation in the central nervous system of virus-infected mice. *J Immunol.* 2005;175:1767–1775.
25. Campanella GS, Tager AM, El Khoury JK, et al. Chemokine receptor CXCR3 and its ligands CXCL9 and CXCL10 are required for the development of murine cerebral malaria. *Proc Natl Acad Sci U S A.* 2008;105:4814–4819.
26. Khan IA, MacLean JA, Lee FS, et al. IP-10 is critical for effector T cell trafficking and host survival in *Toxoplasma gondii* infection. *Immunity.* 2000;12:483–494.
27. Pittet MJ, Mempel TR. Regulation of T-cell migration and effector functions: insights from in vivo imaging studies. *Immunol Rev.* 2008;221:107–129.
28. John B, Harris TH, Tait ED, et al. Dynamic imaging of CD8(+) T cells and dendritic cells during infection with *Toxoplasma gondii*. *PLoS Pathog.* 2009;5:e1000505.
29. Wilson EH, Harris TH, Mrass P, et al. Behavior of parasite-specific effector CD8+ T cells in the brain and visualization of a kinesis-associated system of reticular fibers. *Immunity.* 2009; 30:300–311.
30. Chtanova T, Han SJ, Schaeffer M, et al. Dynamics of T cell, antigen-presenting cell, and pathogen interactions during recall responses in the lymph node. *Immunity.* 2009;31:342–355.
31. Schaeffer M, Han SJ, Chtanova T, et al. Dynamic imaging of T cell-parasite interactions in the brains of mice chronically infected with *Toxoplasma gondii*. *J Immunol.* 2009;182:6379–6393.
32. Crane IJ, Xu H, Wallace C, et al. Involvement of CCR5 in the passage of Th1-type cells across the blood-retina barrier in experimental autoimmune uveitis. *J Leukoc Biol.* 2006;79:435–443.
33. Xu H, Manivannan A, Jiang HR, et al. Recruitment of IFN-gamma-producing (Th1-like) cells into the inflamed retina in vivo is preferentially regulated by P-selectin glycoprotein ligand 1:P/E-selectin interactions. *J Immunol.* 2004;172:3215–3224.
34. Xu H, Forrester JV, Liversidge J, Crane IJ. Leukocyte trafficking in experimental autoimmune uveitis: breakdown of blood-retinal barrier and upregulation of cellular adhesion molecules. *Invest Ophthalmol Vis Sci.* 2003;44:226–234.
35. Xu H, Manivannan A, Liversidge J, Sharp PF, Forrester JV, Crane IJ. Involvement of CD44 in leukocyte trafficking at the blood-retinal barrier. *J Leukoc Biol.* 2002;72:1133–1141.
36. Spencer DB, Lee EJ, Kawaguchi T, Rosenbaum JT. In vivo imaging of the immune response in the eye. *Semin Immunopathol.* 2008; 30:179–190.
37. Mrass P, Takano H, Ng LG, et al. Random migration precedes stable target cell interactions of tumor-infiltrating T cells. *J Exp Med.* 2006;203:2749–2761.
38. Chan-Ling T. Glial, vascular, and neuronal cytogenesis in whole-mounted cat retina. *Microsc Res Tech.* 1997;36:1–16.
39. Elso CM, Roberts LJ, Smyth GK, et al. Leishmaniasis host response loci (lmr1–3) modify disease severity through a Th1/Th2-independent pathway. *Genes Immun.* 2004;5:93–100.
40. Dullforce PA, Seitz GW, Garman KL, et al. Antigen-specific accumulation of naive, memory and effector CD4 T cells during anterior uveitis monitored by intravital microscopy. *Cell Immunol.* 2006;239:49–60.
41. Gazzinelli R, Xu Y, Hieny S, Cheever A, Sher A. Simultaneous depletion of CD4+ and CD8+ T lymphocytes is required to reactivate chronic infection with *Toxoplasma gondii*. *J Immunol.* 1992;149:175–180.
42. Commodaro AG, Belfort RN, Rizzo LV, et al. Ocular toxoplasmosis: an update and review of the literature. *Mem Inst Oswaldo Cruz.* 2009;104:345–350.
43. Norose K, Mun HS, Aosai F, et al. IFN-gamma-regulated *Toxoplasma gondii* distribution and load in the murine eye. *Invest Ophthalmol Vis Sci.* 2003;44:4375–4381.
44. Dustin ML. Multiscale analysis of T cell activation: correlating in vitro and in vivo analysis of the immunological synapse. *Curr Top Microbiol Immunol.* 2009;334:47–70.
45. Dustin ML. Regulation of T cell migration through formation of immunological synapses: the stop signal hypothesis. *Adv Exp Med Biol.* 2002;512:191–201.
46. Muller M, Carter SL, Hofer MJ, et al. CXCR3 signaling reduces the severity of experimental autoimmune encephalomyelitis by controlling the parenchymal distribution of effector and regulatory T cells in the central nervous system. *J Immunol.* 2007;179:2774–2786.
47. Strack A, Asensio VC, Campbell IL, Schluter D, Deckert M. Chemokines are differentially expressed by astrocytes, microglia and

inflammatory leukocytes in *Toxoplasma* encephalitis and critically regulated by interferon-gamma. *Acta Neuropathol.* 2002;103:458–468.

48. Carter SL, Muller M, Manders PM, Campbell IL. Induction of the genes for Cxcl9 and Cxcl10 is dependent on IFN-gamma but shows differential cellular expression in experimental autoimmune encephalomyelitis and by astrocytes and microglia in vitro. *Glia.* 2007;55:1728–1739.
49. Khan IA, Thomas SY, Moretto MM, et al. CCR5 is essential for NK cell trafficking and host survival following *Toxoplasma gondii* infection. *PLoS Pathog.* 2006;2:e49.
50. Caspi R. Autoimmunity in the immune privileged eye: pathogenic and regulatory T cells. *Immunol Res.* 2008;42:41–50.
51. Glabinsk AR, Ransohoff RM. Targeting the chemokine system for multiple sclerosis treatment. *Curr Opin Invest Drugs.* 2001;2:1712–1719.
52. Viola A, Luster AD. Chemokines and their receptors: drug targets in immunity and inflammation. *Annu Rev Pharmacol Toxicol.* 2008;48:171–197.
53. Crane IJ, Wallace CA, McKillop-Smith S, Forrester JV. Control of chemokine production at the blood-retina barrier. *Immunology.* 2000;101:426–433.